Metformin incombination with curcumin inhibits the growth, metastasis, and angiogenesis of hepatocellular carcinoma in vitro and in vivo

Hui-Hui Zhang[1], Ying Zhang[1], Yan-Na Cheng[1], Fu-Lian Gong[1], Zhan-Qi Cao[1], Lu-Gang Yu[2], Xiu-Li Guo[1]

[1]Department of Pharmacology, Key Laboratory of Chemical Biology (Ministry of Education), School of Pharmaceutical Sciences, Shandong University, Jinan, P.R. China.

[2]Department of Gastroenterology, Institute of Translational Medicine, University of Liverpool, Liverpool, UK.

Abstract

Hepatocellular carcinoma (HCC) has poor prognosis due to the advanced disease stages by the time it is diagnosed, high recurrence rates and metastasis. In the present study, we investigated the effects of metformin (a safe anti-diabetic drug) and curcumin (a turmeric polyphenol extracted from rhizome of Curcuma longa Linn.) on proliferation, apoptosis, invasion, metastasis, and angiogenesis of HCC in vitro and in vivo. It was found that co-treatment of metformin and curcumin could not only induce tumor cells into apoptosis through activating the mitochondria pathways, but also suppress the invasion, metastasis of HCC cells and angiogenesis of HUVECs. These effects were associated with downregulation of the expression of MMP2/9, VEGF, and VEGFR-2, up-regulation of PTEN, P53 and suppression of PI3K/Akt/mTOR/NF-κB and EGFR/STAT3 signaling. Co-administration of metformin and curcumin significantly inhibited HCC tumor growth than administration with metformin or curcumin alone in a xenograft mouse model. Thus, metformin and curcumin in combination showed a better anti-tumor effects in hepatoma cells than either metformin or curcumin presence alone and might represent an effective therapeutic strategy for HCC treatment.

1 INTRODUCTION

Hepatocellular carcinoma (HCC) is a leading cause of cancer-related mortality, ranking the fifth most prevalent cancer in the world.[1] Despite significant advances in diagnosis and treatment of HCC, the prognosis of HCC remains poor, largely due to the advanced stages by the time it is diagnosed, high recurrence rates and metastasis.[2] The side effects of chemotherapy agents and drug resistance also remain major concerns of the treatment options.[3] Therefore, new chemotherapeutic strategies focus on the potential agents with fewer side effects to inhibit growth of existing tumors and prevent cancer cells invasion, metastasis, and angiogenesis.[4]

Conventional chemotherapy remains ineffective in curing HCC due to its high hepatotoxicity. Natural dietary phytochemicals could be potential options of cancer therapy for reducing adverse side effects and improving the anti-cancer effectiveness.[5] Curcumin is a turmeric polyphenol extracted from rhizome of

Curcuma longa Linn. Curcumin has pleiotropic pharmacological effects, good tolerance and low toxicity[6] and has been reported to have anti-tumor effects in numerous cancers, including HCC.[7]

Metformin is a well-tolerated anti-diabetic drug and has been reported to reduce the risk of various cancers including HCC.[8] Recently, clinical evaluation of metformin for its chemo-preventive and antineoplastic effects has bypassed the traditional phase I assessment and directly moved to phase II/III trials in several cancers due to its excellent safety record in diabetic patients.[9] Incombination with sorafenib, metformin has been shown to more effectively inhibit cell growth, migration, and invasion of HCC cells than monotherapy with sorefenib alone.[10]

In the present study, we investigated the effects of metformin in combination with curcumin on the proliferation, apoptosis, invasion, metastasis, and angiogenesis of HCC.

2 MATERIALS AND METHODS

2.1 Cell culture and drugs

Metformin and curcumin were purchased from Sigma-Aldrich (St. Louis, MO). They were dissolved in PBS and dimethylsulfoxide (DMSO) with the final concentration of 500 and 50 mM, respectively. The human HCC cell lines HepG2, PLC/PRF/5, and human umbilical vein endothelial cells (HUVECs) were purchased from ATCC (Rockville, MD). The human immortalized normal liver cell line L-02 was purchased from the China Cell Bank (Shanghai, China). The human normal gastric epithelial cell line GES-1 was purchased from Boshun Joint Experiment Center (Shanghai, China). HepG2, PLC/PRF/5, L-02, and HUVEC cells were cultured in Dulbecco's modified Eagle medium (DMEM, Gibco, Grand Island, NY) and GES-1 cells in RPMI-1640 medium (Gibco) supplemented with 10% (v/v) heat-inactivated fetal bovine serum (FBS, Gibco), 100 units/mL penicillin and 100 μg/mL streptomycin (Solarbio technology co., LTD. China) in a humidified 5% CO2 incubator at 37°C.

2.2 Cell proliferation assay

Cell proliferation was measured by 3-(4, 5-Dimethylthiazol-2-yl)-2, 5-diphenyltetrazolium bromide (MTT, Solarbio) assay and cell counting kit-8 (CCK-8, DOJINDO, Kyushu, Japan) assay. For MTT assay, after treatment of the cells with or without metformin and/or curcumin, 10% of MTT solution was added and the absorbance was measured at 570 nm using Thermo Multiskan GO microplate reader (Thermo-1510, CA). CCK-8 assay was performed according to the manufacturer's instructions. Briefly, after treatment of the cells with drugs, 10% of CCK-8 solution was added and the absorbance was measured at 450 nm. The absorbance of untreated cells was considered as 100% cell viability.

2.3 Colony formation assay

After treatment of the cells with metformin and/or curcumin, cells were cultured in drug-free medium for approximate 14 days. The cells were fixed with cold methanol-glacial acetic acid and stained with crystal violet. Total number of colonies that contained more than 50 cells was counted.

2.4 Hoechst 33342 staining assay

After treatment of the cells with metformin and/or curcumin and fixed with cold methanol-glacial acetic acid, the cells were stained with Hoechst 33342 (10 μg/mL) for 20 min and visualized with fluorescence microscope (excitation, 340 nm; emission, 460 nm NIKON, Ti-U, Tokyo, Japan).

2.5 Annexin V-FITC/PI staining assay

After treatment of the cells with metformin and/or curcumin, cells apoptosis was measured by quantitatively determining cell surface phosphatidylserine in apoptotic cells using Annexin V-FITC/PI apoptosis detection kit (4A Biotech, China) and analyzed by a FACScan flow cytometry (Becton Dickinson, Franklin Lakes, NJ), with emission filters of 525 and 575 nm, respectively.

2.6 Cell cycle analysis

After treatment of the cells with metformin and curcumin, cells were harvested and introduced with propidium iodide (PI) for 15 min before analyzed using FACScan flowcytometry. Cell cycle distribution was analyzed using the Modifit's program (Becton Dickinson).

2.7 Mitochondrial membrane potential (ΔΨm) assay

Mitochondrial membrane potential was determined by measuring the potential-dependent accumulation of 5,5′,6,6′-tetrachloro-1,1′3,3′-tetraethyl-benzimidazolylcarbocyanine iodide (JC-1) using the mitochondrial membrane sensor kit (Beyotime, China). After treatment of the cells with metformin and/or curcumin, cells were washed and incubated with JC-1 staining solution according to the manufacturer's instruction before they were harvested and analyzed by flow cytometry.

2.8 Western blot analysis

Proteins were separated by sodium dodecyl sulphate polyacrylamide gel electrophoresis (SDS-PAGE) and transferred onto a polyvinylidene fluoride (PVDF) membrane (Millipore, Billerica, MD). The membranes were washed, blocked with TBST buffer (20 mM Tris-buffered saline and 0.1% Tween-20) containing 5% (w/v) non-fat dry milk overnight before incubated with antibodies against human PI3K (#4255), Akt (#9272), p-Akt (#2965), mTOR (#2972), p-mTOR (#2971), p53 (#9282), PTEN (#9559), Bcl-2 (#2872), Bax (#2772), cleaved-PARP (#9541), MMP2 (#4022), MMP9 (#3852), VEGFR-2 (#2479), EGFR (#2232), p-EGFR (#2235), p-STAT3 (#9145), NF-κB (#4764) (all from Cell Signaling Technology, CST, Boston, MA), VEGF (22341-1-AP, Proteintech, Wuhan, China) and anti-β-actin (ZF-0313, ZS Bio. Beijing, China). All primary antibodies were diluted by 1:1000 in primary antibody diluents. The secondary antibodies used were either goat anti-mouse or goat anti-rabbit IgG (PIERCE, 1:10000 in TBST), depending on the primary antibody used. Antibody bindings were detected by enhanced chemiluminescence reagent (Millipore) and quantified by densitometry using a ChemiDoc XRS + molecular imager (Bio-Rad, Hercules, CA).

2.9 Wound scratch assay

The cell monolayer was scratched to a cell-free approximate 1 mm wound-like gap in 6 well plates using a sterile pipette. After treatment with metformin and curcumin, cell images in the scratch area were captured under the inverted microscope at 100× magnification (NIKON ECLTPSE, Tokyo, Japan). Cell migration was quantified by measuring the width of the cell-free zone (distance between the edges of the injured monolayer).

2.10 Transwell cell migration and matrigel invasion assays

Cell migration and invasion were measured using transwell chambers. For the migration assay, cells suspended in serum-free medium were delivered into the upper compartment of transwell chamber and treated with metformin and/or curcumin. Complete culture medium containing 10% FBS was added to the lower compartment as a chemoattractant. After treatment, the cells remained on the upper surface of the membrane were removed with cotton swabs. Migrated cells to the bottom side of the membrane were fixed by cold methanol-glacial acetic acid and stained with crystal violet, and counted. For the invasion assay, the transwell membrane was first coated with matrigel (BD Biosciences, Bedford, MA), and the rest of procedures were the same as that described above in the migration assay.

2.11 Gelatin zymography protease assay

MMP2 and MMP9 activity in conditional medium was measured by gelatin zymography protease assays as previously described.[11] Briefly, after cell treatment, the supernatant in the culture wells was collected and applied to electrophoresis on SDS-polyacrylamide gel electrophoresis (PAGE) copolymerized

with gelatin as a substrate. Following electrophoresis, the gels were rinsed and incubated in activation buffer (50 mM Tris, 10 mM CaCl2, 1 μM ZnCl2, 200 mM NaCl, pH 7.4) for 16 h before stained with 0.1% Coomassie brilliant blue R-250 and destained in acetic acid. Non-staining regions of the gel corresponding to MMP2 and MMP9 were quantified by densitometry using ChemiDoc XRS + image analyzer (Bio-Rad).

2.12 In vitro angiogenesis assay

The tube formation assay was performed using HUVECs cultured on matrigel. HUVECs (3 × 104 cells/well) were seeded onto 3-D matrigel with or without metformin and/or curcumin for 6 h. The morphogenesis of capillary-like tubes was visualized in a bright field with a microscope (NIKON ECLTPSE). The tube formation was defined by counting the branch points of the formed tubes and average numbers of branch points for each group were calculated.

2.13 In vivo antitumor activity assay

Female Balb/c-nu mice (Animal Centre of China Academy of Medical Sciences, Beijing, China) were housed under pathogen-free conditions. All experimental procedures conformed to the animal experiment guidelines of the Animal Care and Welfare Committee of Shandong University. HepG2 xenografts were established by inoculating 2.0 × 106 HepG2 cells s.c in nude mice. The experiments began when the xenografts volume reached approximately 1.0 cm3 in nude mice. The tumor were extracted and cut into 1 mm3 fragments (about 20 mg/fragment) under a sterile condition. One fragment was transplanted s.c. into the right flank by trocar in each nude mouse.[12] When the tumor volume reached approximate 100 mm3, the mice were randomly divided into four groups (n = 7) and were daily administrated by i.p. injection with vehicle [PEG400: ethanol: dextrose 5% in water (D5W) = 4:1:5, to dissolve curcumin], oral administration of metformin (150 mg/kg), i.p. injection with curcumin (60 mg/kg), oral administration of metformin (150 mg/kg) plus i.p. injection with curcumin (60 mg/kg) for 21 consecutive days. The tumor size and animal body weights were measured every 3 days. Tumor volume (V) is calculated as $V = W2 \times L/2$, where W is width (short axis) and L is length (long axis). At the end of the experiment, the mice were sacrificed and the tumors were removed and weighed. Effect of metformin and curcumin on tumor growth was expressed as percentage to that in the vehicle group.

2.14 Statistical analysis

All experiments were performed at least three times. Data are expressed as mean ± SD and analyzed by one-way analysis of variance (ANOVA). Statistical analysis was performed using the SPSS/Win 13.0 software (SPSS, Inc., Chicago, IL). P value <0.05 is considered statistically significant.

3 RESULTS

3.1 Metformin and curcumin together induces stronger inhibition of HCC cells growth in vitro and in vivo

The presence of metformin and curcumin both showed to cause dose-dependent inhibition of HepG2 and PLC/PRF/5 cells proliferation. The IC50 values of metformin were 53.72 ± 3.40, 23.46 ± 3.45, 8.52 ± 0.93 (mM) and that of curcumin were 22.15 ± 0.51, 15.94 ± 2.06, 9.15 ± 0.20 (μM) for 24, 48, and 72 h, respectively on HepG2 cells (Figures 1A and 1B, Table 1). The IC50 values of metformin were 63.62 ± 2.99, 24.68 ± 0.55, 9.97 ± 0.13 (mM) and that of curcumin were 26.87 ± 2.46, 16.33 ± 0.61, 9.31 ± 0.95 (μM) for 24, 48, and 72 h, respectively on PLC/PRF/5 cells (Figures 2A and 2B, Table 1).

The synergistic effects of metformin and curcumin on HepG2 and PLC/PRF/5 cell growth were confirmed by CCK-8 assay (Figures 1E and 2D) and colony-formation assay (Figures 1F, 1G and 2E, 2F). The combined treatment of metformin and curcumin showed to induce a weak cytotoxicity (<20%) on human normal hepatocytes (L-02), human umbilical vein endothelial cells (HUVECs), and human normal gastric epithelial cells (GES-1) (Figure 1C).

Administration of metformin and curcumin in a mice xenograft model showed to induce significant inhibition of HepG2 tumor growth in mice (Figure 3). In comparison with the vehicle control group, mice in the combined treatment group showed 58.33% reduction of tumor growth, while oral administration of metformin at 150 mg/kg and i.p. injection with curcumin at 60 mg/kg resulted in 24.10 and 31.85% tumor reduction, respectively (Table 3). The tumor suppression effect of metformin in combination with curcumin was also manifested by a slower increase of the tumor volume. No significant differences in the animal weight of body, or other adverse effects were observed among the treated and control groups.

3.2 Metformin and cucumin in combination enhances cell apoptosis in HCC cells through regulation of the mitochondrial-associated apoptosis pathway

Decreased apoptotic activity is one of the most important features of HCC.[15] To investigate effects of a combined treatment of metformin and curcumin on HepG2 or PLC/PRF/5 cell apoptosis, we first examined the cell morphology in cell response to the treatment. Treatment of HepG2 and PLC/PRF/5 cells with metformin and curcumin followed by nucleus staining with Hoechst 33342 showed increased number of cells with reduced nuclear size, chromatin condensation, nuclear fragmentation, and appearance of apoptotic bodies, characteristics of apoptosis in comparison to the cells treated with metformin or curcumin alone (Figures 4A and 5A).

Annexin V cell surface staining also showed significant increase of Annexin V positive cells following treatment with the combination therapy in comparison to monotherapy. As illustrated in Figures 4B and 5B, the presence of 10 mM metformin significantly enhanced the apoptotic effects of curcumin at 5 or 10 μM from

10.81 ± 0.55% to 25.04 ± 1.32% or from 13.84 ± 0.48% to 36.23 ± 2.43% in HepG2 cells, and from 6.90 ± 0.62% to 17.00 ± 1.30% or from 11.15 ± 0.36% to 26.02 ± 2.91% in PLC/PRF/5 cells, respectively. These results indicated that the presence of metformin increased apoptosis of HepG2 and PLC/PRF/5 cells induced by curcumin.

As mitochondrion is an important organelle in apoptosis initiation in response to stress, we assessed the mitochondrial function by measuring mitochondrial transmembrane potential (ΔΨm) using JC-1 staining in cells response to metformin and curcumin. Metformin presence further enhanced the reduction in mitochondrial membrane potential by curcumin in HepG2 cells (Figure 4D). Combination treatment of metformin with curcumin also increased the expression of Bax (pro-apoptotic member), with concurrent suppression of Bcl-2 (anti-apoptotic member) and up-regulation of cleaved PARP. The Bax to Bcl-2 ratio was seen to be increased by combination treatment compared with curcumin alone in both HepG2 cells and xenografts (Figures 4C and 4E). These results indicate that the combined treatment of metformin and curcumin evoked mitochondrial dysfunction-related apoptosis in HepG2 cells. It is noted that the combined treatment of metformin and curcumin also induced G2/M phase arrest concomitant with a decrease in G0/G1 and S phase in HepG2 and PLC/PRF/5 cells (Figures 4F and 5C).

3.3 Combined treatment with metformin and curcumin inhibited migration and invasion of HCC cells by reducing MMP2 and MMP9 expression and activity

In comparison to untreated cells, the presence of metformin at 2.5 and 5 mM and curcumin at 2.5 and 5 μM had no significant effect on HepG2 cell proliferation (Figure 6E). Therefore, these concentrations of metformin and curcumin were used in subsequent experiments as the maximum non-cytotoxic concentrations of the drugs.

In the wound healing assay, co-presence of metformin and curcumin in the culture resulted in slower closure of the gaps than the presence of metformin or curcumin alone. The inhibition of migration by curcumin (2.5, 5 μM) was further increased by the presence of metformin (5 mM) from 12.69 ± 0.34% to 39.44 ± 2.10%, from 23.92 ± 4.56% to 52.12 ± 2.08% at 12 h, from 15.03 ± 0.76% to 49.25 ± 2.94%, from 28.30 ± 3.04% to 63.27 ± 3.34% at 24 h, respectively (Figure 6A). In the cell motility assay, HepG2 and PLC/PRF/5 cells in the vehicle control group displayed high invasive and migrated ability. The activity of invasion and migration of HepG2 and PLC/PRF/5 cells was markedly suppressed by exposure to metformin and curcumin. Metformin (5 mM) enhanced the inhibition rate of migration induced by curcumin from 23.94 ± 0.72% to 67.92 ± 1.54% (2.5 μM), from 57.80 ± 2.20% to 79.83 ± 2.58% (5 μM) (Figure 6C), and potentiated the inhibition rate of invasion from 34.79 ± 4.46% to 77.09 ± 5.76% (2.5 μM), from 56.57 ± 3.92% to 88.13 ± 4.25% (5 μM) (Figure 6D), respectively on HepG2 cells. The same results were confirmed by PLC/PRF/5 cells. The presence of 5 mM metformin significantly enhanced the inhibitory effect of migration of curcumin at 2.5 or 5 μM from 11.20 ± 2.41% to 47.70 ± 1.69%, or from 38.21 ± 2.15% to 65.51 ± 5.49% (Figure 5D), and potentiated the inhibitory effect of invasion of curcumin at 2.5 or 5 μM from 19.03 ± 3.45% to 51.97 ± 1.64%, or from

41.44 ± 4.24% to 73.91 ± 1.55% (Figure 5E), respectively on PLC/PRF/5 cells. These results further confirm that a combined treatment with metformin and curcumin inhibits migration and invasion of HepG2 or PLC/PRF/5 cells.

To test whether MMP2 and MMP9 (well-known pro-proliferation/metastasis proteins)[16] were involved in metformin and curcumin-mediated cell migration and invasion, gelatin zymography was performed. As shown in Figure 6G, the activity of MMP9 and MMP2 was suppressed by co-presence of metformin with curcumin. Co-presence of metformin and curcumin also showed to inhibit the expression of active MMP9 and MMP2 in HepG2 cells (Figure 6H) and xenografts (Figure 6F). These indicate that one of the possible mechanisms responsible for the inhibitory effects of metformin and curcumin on the migration and invasion of HepG2 cells is related to down-regulation of MMP9 and MMP2 expression and activity.

3.4 Combined treatment with metformin and curcumin suppresses migration and capillary tube formation of HUVECs

At non-toxic concentrations, metformin (10 mM) and curcumin (5, 10 μM) caused significant reduction in the number and the continuity of HUVEC capillary-like structures in a dose-dependent manner in vitro (Figures 1C and 6I). Moreover, co-presence of metformin and curcumin significantly inhibited the HUVEC cell migration in comparison to the presence of curcumin alone ($P < 0.01$) (Figure 6B). These data indicated that curcumin in combination with metformin has stronger effect on inhibition of endothelial cell migration and tubule formation in angiogenesis.

3.5 Combined treatment of metformin and curcumin downregulates PTEN/PI3K/Akt/mTOR/NF-κB and EGFR/VEGF/VEGFR-2/STAT3 signaling in HepG2 cells

Activation of the PI3K/Akt/mTOR signaling pathway is known to be involved in regulating tumor cell invasion and metastasis in response to various growth factors in HCC.[17] As shown in Figure 7A–C, metformin could significantly decrease the expression of PI3K and phospho-Akt. Curcumin could dramatically inhibit the expression of phospho-mTOR and increase the expression of PTEN. Interestingly, a synergistic down-regulation of PI3K, phospho-Akt, and phospho-mTOR was observed with combined treatment, especially at the combination of 10 mM metformin with 10 μM curcumin. Co-presence of metformin and curcumin significantly increased the expression of PTEN and p53 compared to the untreated cells. NF-κB is a common transcription factor that is related to many signal transduction pathways in cell proliferation, metastasis, and angiogenesis.[18] Treatment of HepG2 cells with metformin reduced the presence of NF-κB in the nucleus and combination treatment of metformin and curcumin together induced stronger inhibition effect (Figure 7D). These results indicated that metformin could inhibit PI3K, phospho-Akt, and NF-κB and curcumin could suppress the phospho-mTOR and activate the PTEN. Metformin in combination with curcumin synergistically inhibits PTEN/PI3K/Akt/mTOR signaling and also suppresses NF-κB nuclear translocation, which confirmed in HepG2 xenografts (Figures 7G and 7H).

To further elucidate the underlying molecular mechanism of metformin and curcumin on angiogenesis, the expressions of EGFR/VEGF/VEGFR-2/STAT3 were also determined upon cell treatment. Co-treatment of HepG2 cells with metformin and curcumin led to dose-dependent decreases of VEGF, VEGFR-2, EGFR, and p-EGFR protein levels (Figures 7E and 7F). Curcumin treatment significantly inhibited the expression of phospho-STAT3 and co-presence of metformin and curcumin induced a synergic inhibition on phospho-STAT3 activation (Figure 7F). Furthermore, the expression of VEGF in HepG2 xenografts was dramatically inhibited by this combination treatment (Figure 7I). These indicates that metformin in combination with curcumin inhibits VEGF expression, an effect that is possibly associated with inhibition of STAT3.

4 DISCUSSION

Over the past years, preclinical and clinical evidence has accumulated that pharmacological inhibition of single targets will induce clinically relevant responses only in a minority of cancer patients and most patients eventually relapsed after treatment.[19] This might be due to intrinsic resistance of cancer cells,[20] as well as feedback mechanisms and redundancy among signaling pathways, alleviating the drug effect,[19] which crucially contributed to the high mortality of liver cancer.[21] In order to improve survival rate, the therapeutic strategies based on the combination of two types of drugs by regulating one or more mechanisms of carcinogenesis are attractive.[22] This study demonstrated that co-presence of metformin and curcumin induced stronger activation of HCC cell apoptosis and stronger inhibition of tumor cell growth and metastasis in vitro and in vivo than either metformin or curcumin alone.

The challenge of conventional chemotherapy in hepatic cancer is unavoidable toxicity to normal human cells especially hepatic epithelial cells. The present data showed that metformin and curcumin in combination produced higher cytotoxicity to HCC including HepG2 cells or PLC/PRF/5 cells than to non-tumor cells including normal liver cells (L-02), human umbilical vein endothelial cells (HUVECs) and normal gastric epithelial cells (GES-1). Co-administration of 150 mg/kg metformin and 60 mg/kg curcumin per mice, which was equivalent to about 645 and 225 mg dose in a 60 kg human, respectively, significantly suppressed HCC growth in mice without any obvious side effects. The low cytoxcicity and strong anti-cancer effect is an indication of potentially effective use of these two drugs in combination for HCC treatment. However, we will do further evaluation on the synergistic effects of this combination therapy against hepatoma using other liver cancer animal models such as orthotopic HCC mouse model or spontaneous mouse liver cancer, etc.

Many chemotherapeutic agents have been shown to induce cell apoptosis.[23] Apoptosis can be activated through extrinsic or intrinsic signaling pathways.[24] Bax and Bcl-2 are important regulators of the mitochondrial-associated intrinsic apoptosis

signaling pathway. They reduce the mitochondrial membrane potential to cause outer mitochondrial membrane permeabilization leading to mitochondrial release of caspase-activating cytochrome C in apoptosis activation.[25] It is know that Bax and Bc1-2 can be activated by tumor suppresser p53 in apoptosis.[26] The apoptosis evoked by metformin and curcumin is shown in this study to be associated with activation of p53, increased Bax/Bcl-2 ratio and increased cleavage of PARP, suggesting the apoptosis-induction of metformin and curumin is involved in activation of mitochondrial-associated intrinsic apoptosis signaling.

PI3K/Akt/mTOR signaling plays an important role in the regulation of tumor growth, apoptosis, metabolism, angiogenesis, invasion, and metastasis.[17, 27] PI3K/Akt activation can stimulate anti-apoptotic proteins (such as Bcl-2) and also inhibit some pro-apoptotic proteins (such as Bax, caspase, and p53), preventing the release of apoptosis-stimulating factors from mitochondria.[28] PTEN, a tumor suppressor gene, is a negative regulator of the PI3K/Akt signaling. PTEN suppression is associated with increased metastasis, aggressive tumor growth, and poor prognosis of HCC.[29] In this study, metformin could inhibit PI3K and phospho-Akt, and curcumin could suppress the phospho-mTOR and activate the PTEN. The presence of metformin with curcumin could synergistically down-regulate the expressions of PI3K, p-AKT, and p-mTOR and up-regulate the expression of PTEN. These discoveries are in keeping with the tumor cell growth inhibitory effect of metformin and curcumin shown in vitro and in vivo.

Activation of PI3K/Akt singaling has been reported to enhance MMP2 and MMP9 expression in HCC through activation of NF-κB[30] and promote HCC cell invasion and metastasis.[31] MMPs, particularly MMP2 and MMP9, have long been associated with high metastatic potential of HCC.[16] In this study, we found that the presence of metformin and curcumin reduced Akt phosphorylation, inhibited NF-kB nuclear translocation and decreased MMP2 and MMP9 expression and activity in HepG2 cells. These findings indicate that the strong inhibitory effect of metformin and curcumin in combination on HCC cell migration and invasion is associated with activation of the PI3 K/Akt/NF-κB/MMP2/9 signaling.

Angiogenesis plays a critical role in tumor growth, invasion and metastasis by providing essential growth required nutrients and oxygen.[32] Vascular endothelial growth factor (VEGF) is a key angiogenesis promoter[33] and can also be used as a tumor marker.[34] A number of studies have shown that VEGF expression is elevated in HCC vascular endothelial cells in comparison to that in normal tissues.[35] HCC patients with high VEGF expression had a higher recurrence rate and poorer prognosis than those with low VEGF expression.[36] VEGFR-2 is the primary receptor of VEGF in its proangiogenic activity.[37] PI3K/Akt/NF-κB pathway can regulate the invasion of carcinoma cells, featured with the up-regulation of VEGF, suggesting the critical role of VEGF as the downstream target of

PI3K/Akt/NF-κB in mediating cancer invasion and metastasis.[38, 39] STAT3 phosphorylation plays a critical role in the proliferation and survival of various tumor cells and constitutive STAT3 activity up-regulates VEGF expression and tumor angiogenesis.[40] EGFR, an important STAT3-related factor, is associated with the proliferation activity, stage, carcinoma differentiation, invasiveness, and recurrence and it is proposed to play an important role in carcinogenesis and HCC progression.[41]

5 **CONCLUSION**

In conclusion, metformin and curcumin in combination induces cell apoptosis and inhibits tumor growth of HCC through at least two or three mechanisms (Figure 8). It enhances the expression of Bax/Bcl-2 ratio by activation of cellular p53 thus promotes cell apoptosis. It suppress the nuclear translocation of NF-κB, leading to inhibition of MMP2/9 expression and also to suppression of the expression and activity of pro-angiogenic factor VEGF and VEGFR-2 which may also involves EGFR/STAT3 activation. Metfomin and curcumin in combination also down-regulates the expression of PI3K, p-Akt, and p-mTOR and increases the expression of PTEN, resulting in suppression of PTEN/PI3K/Akt/mTOR signaling in cell proliferation. A combined therapy of metformin with curcumin might therefore be an effective therapeutic strategy for HCC treatment.

ACKNOWLEDGMENTS

This work was funded by the National Science Foundation of China Grants (81373450), the Major Project of Science and Technology of Shandong Province (2015ZDJS04001, 2015ZDXX0301A03), and from China Australia Centre for Health Science Research (2014GJ03).

CONFLICTS OF INTEREST: Authors declare no conflicts of interest.

References

Torre LA, Bray F, Siegel RL, Ferlay J, Lortet-Tieulent J, Jemal A. Global cancer statistics. CA Cancer J Clin. 2012; 65:87–108.

Lu X, Zhao H, Yang H, et al. A prospective clinical study on early recurrence of hepatocellular carcinoma after hepatectomy. J Surg Oncol. 2009; 100:488–493.

Drews RE, Shulman LN. Update in hematology and oncology. Ann Intern Med. 2010; 152:655–662.

Bruix J, Gores GJ, Mazzaferro V. Hepatocellular carcinoma: clinical frontiers and perspectives. Gut. 2014; 63:844–855.

Sak K. Chemotherapy and dietary phytochemical agents. Chemother Res Pract. 2012; 2012:282570.

Guo Y, Shu L, Zhang C, Su ZY, Kong AN. Curcumin inhibits anchorage-independent growth of HT29 human colon cancer cells by targeting epigenetic restoration of the tumor suppressor gene DLEC1. Biochem Pharmacol. 2015; 94:69–78.

Ma J, Fang B, Zeng F, et al. Curcumin inhibits cell growth and invasion through up-regulation of miR-7 in pancreatic cancer cells. Toxicol Lett. 2014; 231:82–91.

Donadon V, Balbi M, Mas MD, Casarin P, Zanette G. Metformin and reduced risk of hepatocellular carcinoma in diabetic patients with chronic liver disease. Liver Int. 2010; 30:750–758.

Hadad SM, Coates P, Jordan LB, et al. Evidence for biological effects of metformin in operable breast cancer: biomarker analysis in a pre-operative window of opportunity randomized trial. Breast Cancer Res Treat. 2015; 150:149–155.

Hsieh S-C, Tsai J-P, Yang S-F, Tang M-J, Hsieh Y-H. Metformin inhibits the invasion of human hepatocellular carcinoma cells and enhances the chemosensitivity to sorafenib through a downregulation of the ERK/JNK-mediated NF-κB-dependent pathway that reduces uPA and MMP-9 expression. Amino Acids. 2014; 46:2809–2822.

Tang L, Ma X, Tian Q, et al. Inhibition of angiogenesis and invasion by DMBT is mediated by downregulation of VEGF and MMP-9 through Akt pathway in MDA-MB-231 breast cancer cells. Food Chem Toxicol. 2013; 56:204–213.

Xiong X, Fu L, Wang L, et al. Antitumor activity of a novel EGFR tyrosine kinase inhibitor against human lung carcinoma in vitro and in vivo. Invest New Drugs. 2009; 27:1–11.

Chou TC. Theoretical basis, experimental design, and computerized simulation of synergism and antagonism in drug combination studies. Pharmacol Rev. 2006; 58:621–681.

Tahir AA, Sani NF, Murad NA, Makpol S, Ngah WZ, Yusof YA. Combined ginger extract & Gelam honey modulate Ras/ERK and PI3K/AKT pathway genes in colon cancer HT29 cells. Nutr J. 2015; 14:31.

Fabregat I. Dysregulation of apoptosis in hepatocellular carcinoma cells. World J Gastroenterol. 2009; 15:513–520.

Chen JS, Huang XH, Wang Q, et al. Sonic hedgehog signaling pathway induces cell migration and invasion through focal adhesion kinase/AKT signaling-mediated activation of matrix metalloproteinase (MMP)-2 and MMP-9 in liver cancer. Carcinogenesis. 2013; 34:10–19.

Zhang Y, Wang SJ, Han ZH, et al. PI3 K/AKT signaling pathway plays a role in enhancement of eNOS activity by recombinant human angiotensin converting enzyme 2 in human umbilical vein endothelial cells. Int J Clin Exp Pathol. 2014; 7:8112–8117.

Luo H, Rankin GO, Juliano N, Jiang BH, Chen YC. Kaempferol inhibits VEGF expression and in vitro angiogenesis through a novel ERK-NFkappaB-cMyc-p21 pathway. Food Chem. 2012; 130:321–328.

Wu M, Sirota M, Butte AJ, Chen B. Characteristics of drug combination therapy in oncology by analyzing clinical trial data on ClinicalTrials.gov. Pac Symp Biocomput. 2015:68–79.

Di Nicolantonio F, Arena S, Tabernero J, et al. Deregulation of the PI3K and KRAS signaling pathways in human cancer cells determines their response to everolimus. J Clin Invest. 2010; 120:2858–2866.

Rexer BN, Ham AJ, Rinehart C, et al. Phosphoproteomic mass spectrometry profiling links Src family kinases to escape from HER2 tyrosine kinase inhibition. Oncogene. 2011; 30:4163–4174.

Gupta SC, Kannappan R, Reuter S, Kim JH, Aggarwal BB. Chemosensitization of tumors by resveratrol. Ann N Y Acad Sci. 2011; 1215:150–160.

Schwartz GK, Shah MA. Targeting the cell cycle: a new approach to cancer therapy. J Clin Oncol. 2005; 23:9408–9421.

Hassan M, Watari H, AbuAlmaaty A, Ohba Y, Sakuragi N. Apoptosis and molecular targeting therapy in cancer. BioMed Res Int. 2014; 2014:150845.

Breckenridge DG, Xue D. Regulation of mitochondrial membrane permeabilization by BCL-2 family proteins and caspases. Curr Opin Cell Biol. 2004; 16:647–652.

Zheng JH, Viacava Follis A, Kriwacki RW, Moldoveanu T. Discoveries and controversies in BCL-2 protein-mediated apoptosis. FEBS J. 2016; 283:2690–2700.

Saxena NK, Sharma D, Ding X, et al. Concomitant activation of the JAK/STAT, PI3K/AKT, and ERK signaling is involved in leptin-mediated promotion of invasion and migration of hepatocellular carcinoma cells. Cancer Res. 2007; 67:2497–2507.

Seo BR, Min KJ, Cho IJ, Kim SC, Kwon TK. Correction: curcumin significantly enhances dual PI3K/Akt and mTOR inhibitor NVP-BEZ235-induced apoptosis in human renal carcinoma Caki cells through down-regulation of p53-dependent Bcl-2 expression and inhibition of mcl-1 protein stability. PLoS ONE. 2016; 11:e0151886.

Sze KM, Wong KL, Chu GK, Lee JM, Yau TO, Ng IO. Loss of phosphatase and tensin homolog enhances cell invasion and migration through AKT/Sp-1 transcription factor/matrix metalloproteinase 2 activation in hepatocellular carcinoma and has clinicopathologic significance. Hepatology (Baltimore, Md). 2011; 53:1558–1569.

Li J, Lau GK, Chen L, et al. Interleukin 17A promotes hepatocellular carcinoma metastasis via NF-kB induced matrix metalloproteinases 2 and 9 expression. PLoS ONE. 2011; 6:e21816.

Lou L, Ye W, Chen Y, et al. Ardipusilloside inhibits survival, invasion and metastasis of human hepatocellular carcinoma cells. Phytomedicine. 2012; 19:603–608.

Lin D, Wu J. Hypoxia inducible factor in hepatocellular carcinoma: a therapeutic target. World J Gastroenterol. 2015; 21:12171–12178.

Silva SR, Bowen KA, Rychahou PG, et al. VEGFR-2 expression in carcinoid cancer cells and its role in tumor growth and metastasis. Int J Cancer. 2011; 128:1045–1056.

Kammerer PW, Koch FP, Schiegnitz E, et al. Associations between single-nucleotide polymorphisms of the VEGF gene and long-term prognosis of oral squamous cell carcinoma. J Oral Pathol Med. 2013; 42:374–381.

Ranieri G, Ammendola M, Marech I, et al. Vascular endothelial growth factor and tryptase changes after chemoembolization in hepatocarcinoma patients. World J Gastroenterol. 2015; 21:6018–6025.

Deli G, Jin CH, Mu R, et al. Immunohistochemical assessment of angiogenesis in hepatocellular carcinoma and surrounding cirrhotic liver tissues. World J Gastroenterol. 2005; 11:960–963.

Olsson AK, Dimberg A, Kreuger J, Claesson-Welsh L. VEGF receptor signalling—in control of vascular function. Nat Rev Mol Cell Biol. 2006; 7:359–371.

Shen K, Ji L, Gong C, et al. Notoginsenoside Ft1 promotes angiogenesis via HIF-1alpha mediated VEGF secretion and the regulation of PI3 K/AKT and Raf/MEK/ERK signaling pathways. Biochem Pharmacol. 2012; 84:784–792.

Naugler WE, Karin M. NF-kappaB and cancer-identifying targets and mechanisms. Curr Opin Genet Dev. 2008; 18:19–26.

Jung JE, Lee HG, Cho IH, et al. STAT3 is a potential modulator of HIF-1-mediated VEGF expression in human renal carcinoma cells. FASEB J. 2005; 19:1296–1298.

Lee TY, Kim KT, Han SY. Expression of ErbB receptor proteins and TGF-alpha during diethylnitrosamine-induced hepatocarcinogenesis in the rat liver. Korean J Hepatol. 2007; 13:70–80.

Figure legends

Fig 1. Effect of metformin and curcumin, alone and in combination, on HepG2 cell proliferations in vitro. Presence of metformin (A), curcumin (B) or in combination (D) for 24, 48, 72 h on HepG2 cell proliferation was determined by MTT assay. The cytotoxicity effect of combination treatment of metformin and curcumin on HepG2 cells was also evaluated by CCK-8 assay (E). Effects on the colony formation in HepG2 cells were determined for 24 h (F) and for 48 h (G), colonies greater than 50 cells were counting under the dissecting microscope. The cytotoxicity of the treatment on human normal hepatocytes (L-02), human umbilical vein endothelial cells (HUVECs) and human normal gastric epithelial cells (GES-1) for 24 h was investigated by MTT assay (C). Data are presented as the mean ± SD from three independent experiments. *P < 0.05 and **P < 0.01 versus vehicle group, #P < 0.05 and ##P < 0.01

Fig 2. Effect of metformin and curcumin, alone and in combination, on PLC/PRF/5 cell proliferations in vitro. Presence of metformin (A), curcumin (B), or in combination (C) on PLC/PRF/5 cell proliferation for 24, 48, 72 h was determined by MTT asssay. The cytotoxicity effect of combination treatment of metformin and curcumin on PLC/PRF/5 cells was also evaluated by CCK-8 assay (D). Effects on the colony formation in PLC/PRF/5 cells were determined for 24 h (E) and for 48 h (F), colonies greater than 50 cells were counting under the dissecting microscope. Data are presented as the mean ± SD from three independent experiments. *P < 0.05 and **P < 0.01 versus vehicle group, #P < 0.05 and ##P < 0.01 versus curcumin alone group

Fig 3. Effects of metformin and curcumin, alone and in combination, on HepG2 cells growth in vivo mouse xenografts. HepG2 cells were injected s.c. into the right anterior flank of nude mice as described in “Materials and methods.” Mice were treated every day with i.p. curcumin, oral administration of metformin or both agents for 21 consecutive days. Images of mice and subcutaneous tumors derived from the HepG2 xenografts are shown in A and B and tumor weights were shown in C. The body weights (D) and tumor volumes (E) were measured every 3 days. Data are presented as mean ± SD (n = 7). *P < 0.05 and **P < 0.01 versus vehicle group, #P < 0.05 versus curcumin alone group

Fig 4. Effects of metformin and curcumin, alone and in combination, on HepG2 cell apoptosis. HepG2 cells were treated with or without metformin and/or curcumin for 48 h. A: The cells were fixed and stained with DNA-binding fluorochrome Hoechst 33342 for 15 min before visualized with fluorescence microscope (346/460 nm, 200×). Arrows indicate characteristic apoptotic cells. Scale bar = 20 μm. After treatment, annexin-V cell surface binding was analyzed by flow cytometry. Q1-LL, LR, UR, and UL represent normal cells, early apoptotic cells, late apoptotic cells and necrotic cells, respectively. The percentages of apoptotic cells (both early and late) in three separate experiments were shown (B). D: After treatment, HepG2 cells were stained for JC-1 and analyzed by flow cytometry. The mitochondrial transmembrane potential (ΔΨm) was measured by detecting the potential-dependent accumulation of JC-1. F: Cell cycle distribution was analyzed by flow cytometry following PI staining.

The expressions of cleaved-PARP, Bcl-2, and Bax in the cells (C) and the expressions of Bcl-2 and Bax in HepG2 xenografts (E) were determined by Western blotting. The protein bands were quantified by densitometry scanning and normalization to β-actin. Data are presented as mean ± SD from three independent experiments. *P < 0.05 and **P < 0.01 versus vehicle group, #P < 0.05 and ##P < 0.01 versus curcumin alone group

Fig 5. Effects of metformin and curcumin, alone and in combination, on PLC/PRF/5 cell apoptosis, invasion, and migration. A: PLC/PRF/5 cells were fixed and stained with DNA-binding fluorochrome Hoechst 33342 for 15 min before visualized with fluorescence microscope (346/460 nm, 200×). Arrows indicate characteristic apoptotic cells. Scale bar = 20 μm. After treatment, annexin-V cell surface binding was analyzed by flow cytometry. Q1-LL, LR, UR, and UL represent normal cells, early apoptotic cells, late apoptotic cells, and necrotic cells, respectively. The percentages of apoptotic cells (both early and late) in three separate experiments were shown (B). Cell cycle distribution was analyzed by flow cytometry following PI staining (C). Migration or invasion of PLC/PRF/5 cells to the bottom side of transwell membrane non-coated (D) or coated with Matrigel (E) after incubation with metformin and curcumin for 24 h were counted by staining with crystal violet. Data are expressed as a percentage to that in the control wells and are presented as mean ± SD from three independent experiments. *P < 0.05 and **P < 0.01 versus vehicle group, #P < 0.05 and ##P < 0.01 versus curcumin alone group

Fig 6. Effect of metformin and curcumin, alone and in combination, on HUVEC tubule formation and HepG2 cell invasion and migration. Sub-cytotoxic concentrations of metformin and curcumin in HepG2 cells were determined using MTT assay (E). Migration of HepG2 (A) and HUVECs (B) in response to metformin and curcumin treatment was determined by wound scratch assay at 0, 12, and 24 h under microscope using an ocular grid (100×). The cell migration ability was quantified by measuring the distance of the scratch front. Migration or invasion of HepG2 cells to the bottom side of transwell membrane non-coated (C) or Matrigel-coated (D) after incubation with metformin and curcumin for 24 h were counted by staining with crystal violet. Data are expressed as a percentage to that in the control wells and are presented as mean ± SD from three independent experiments. Activity of MMP2 and MMP9 in HepG2 cells was estimated by gelatin zymography analysis after treatment with metformin and curcumin for 24 h (G). The expression of MMP2 and MMP9 in HepG2 cells (H) or in xenografts (F) was measured by Western blotting. Effects of metformin (10 mM) and curcumin (5,10 μM) on HUVEC tube formation on Matrigel after 6 h were recorded in bright filed with a fluorescence microscope (100×) (I). Data are presented as the mean ± SD from three independent experiments. *P < 0.05 and **P < 0.01 versus vehicle group, #P < 0.05 and ##P < 0.01 versus curcumin alone group

Fig 7. Effect of metformin and curcumin, alone and in combination, on PTEN/PI3K/Akt/mTOR/NF-κB and VEGF/VEGFR-2/EGFR/STAT3 signaling in HepG2 cells and xenografts. The cellular expression of PI3K, Akt, p-Akt, mTOR, and p-mTOR after treatment with metformin and curcumin in HepG2 cells (A,B) and xenografts (G,H) were measured by Western blotting. Co-treatment with metformin

and curcumin significantly increased the expression of PTEN and p53 (C,H), reduced the expression of NF-κB in the nucleus and cytoplasm (D), and decreased the expressions of VEGF, VEGFR2, EGFR, p-EGFR, and p-STAT3 (E,F,I). Data are presented as mean ± SD from three independent experiments. *P < 0.05 and **P < 0.01 versus vehicle group, #P < 0.05 and ##P < 0.01 versus curcumin alone group. β-actin was used as a loading control

Fig 8. It was found in this study that co-presence of metformin and curcumin strongly inhibited the expression of VEGF, VEGFR-2, EGFR, and p-EGFR. Metformin treatment inhibited NF-κB nuclear translocation and curcumin treatment significantly inhibited the expression of phospho-STAT3. Furthermore, co-presence of metformin and curcumin induced a synergic inhibition effect. The present data suggest that the anti-angiogenic activity of metformin and curcumin in HepG2 cells may be mediated, at least in part, by preventing STAT3 activation, subsequent decreasing VEGF expression. Impeding Akt activity likewise reduces NF-κB levels, subsequently dropping VEGF production and obstructing angiogenesis. Considering all the evidence, our results indicated that metformin and curcumin treatment inhibited tumor angiogenesis and metastasis of HCC through PI3K/Akt/NF-κB and VEGF/VEGFR-2/EGFR/STAT3 pathway.

Fig 1

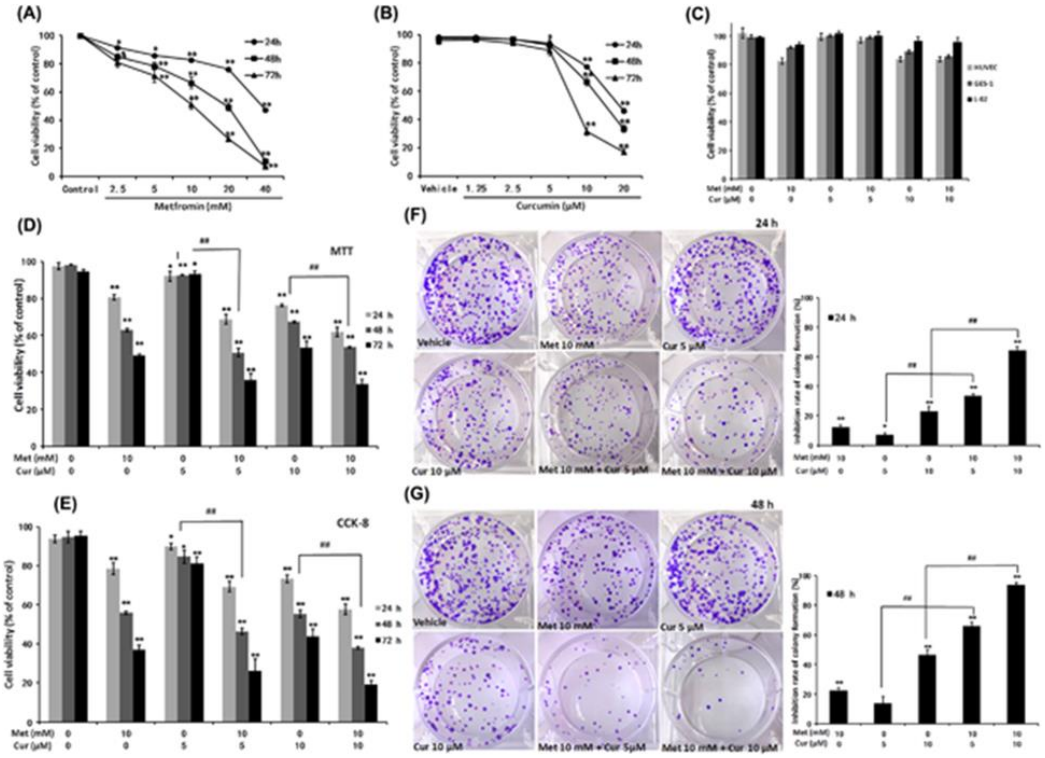
(A)
(B)
(C)
(D)
(E)
(F)
(G)
MTT
CCK-8
24 h
48 h
Vehicle
Met 10 mM
Cur 5 μM
Cur 10 μM
Met 10 mM + Cur 5 μM
Met 10 mM + Cur 10 μM

Fig 2

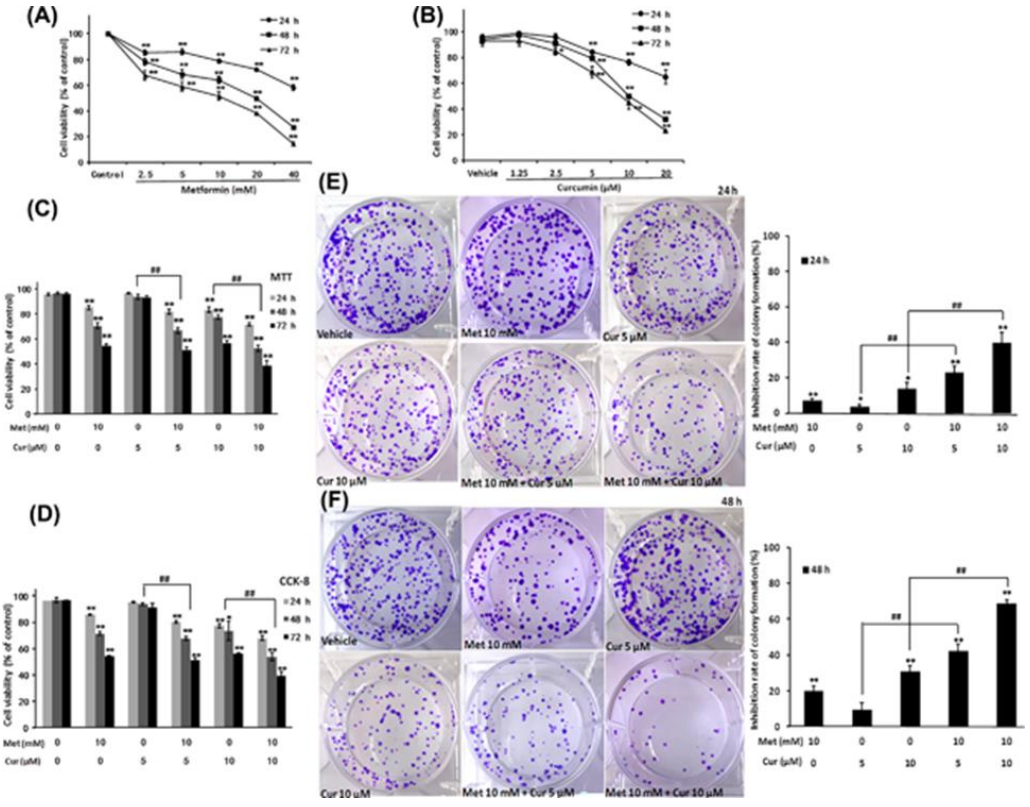
(A)
(B)
(C)
(D)
(E)
(F)
MTT
CCK-8
24 h
48 h
Vehicle
Met 10 mM
Cur 5 μM
Cur 10 μM
Met 10 mM + Cur 5 μM
Met 10 mM + Cur 10 μM

Fig 3

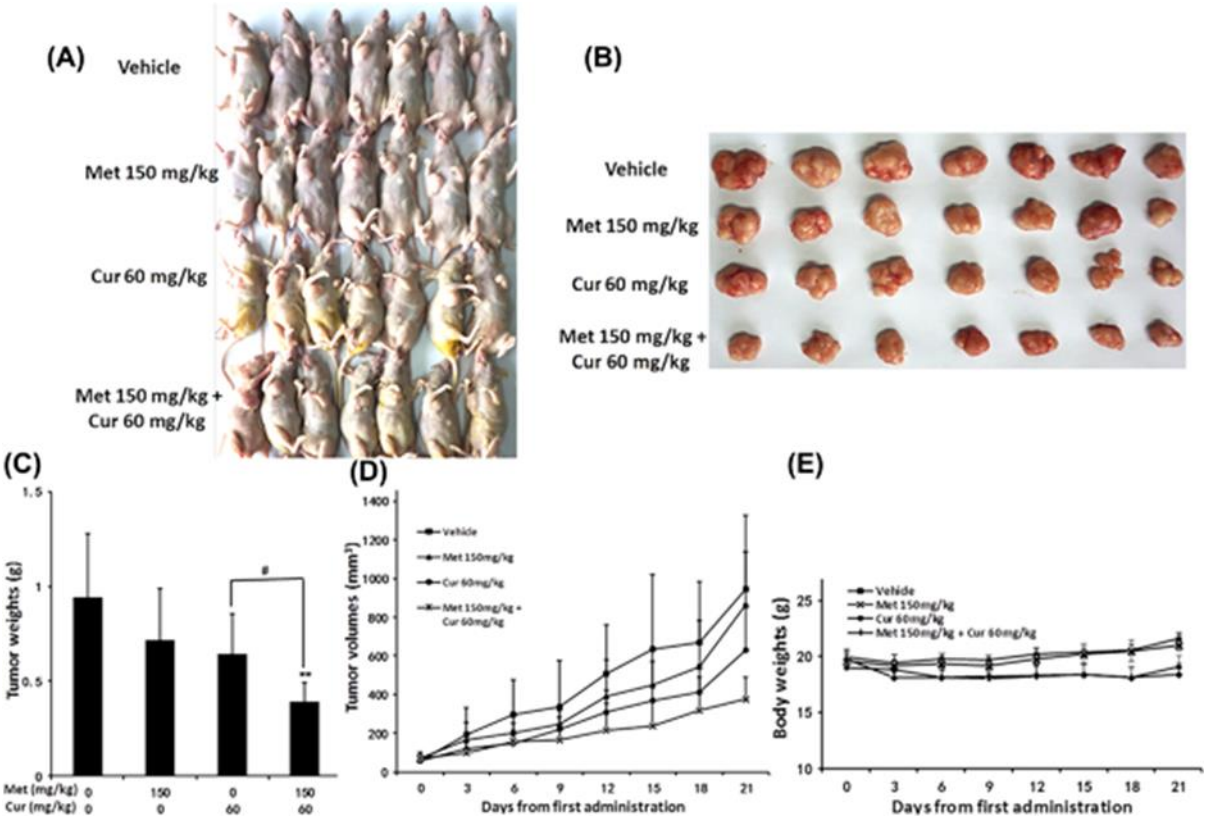
(A)
Vehicle
Met 150 mg/kg
Cur 60 mg/kg
Met 150 mg/kg +
Cur 60 mg/kg
(B)
Vehicle
Met 150 mg/kg
Cur 60 mg/kg
Met 150 mg/kg +
Cur 60 mg/kg
(C)
Tumor weights (g)
Met (mg/kg)
Cur (mg/kg)
(D)
Tumor volumes (mm³)
Vehicle
Met 150mg/kg
Cur 60mg/kg
Met 150mg/kg +
Cur 60mg/kg
Days from first administration
(E)
Body weights (g)
Vehicle
Met 150mg/kg
Cur 60mg/kg
Met 150mg/kg + Cur 60mg/kg
Days from first administration

Fig 4

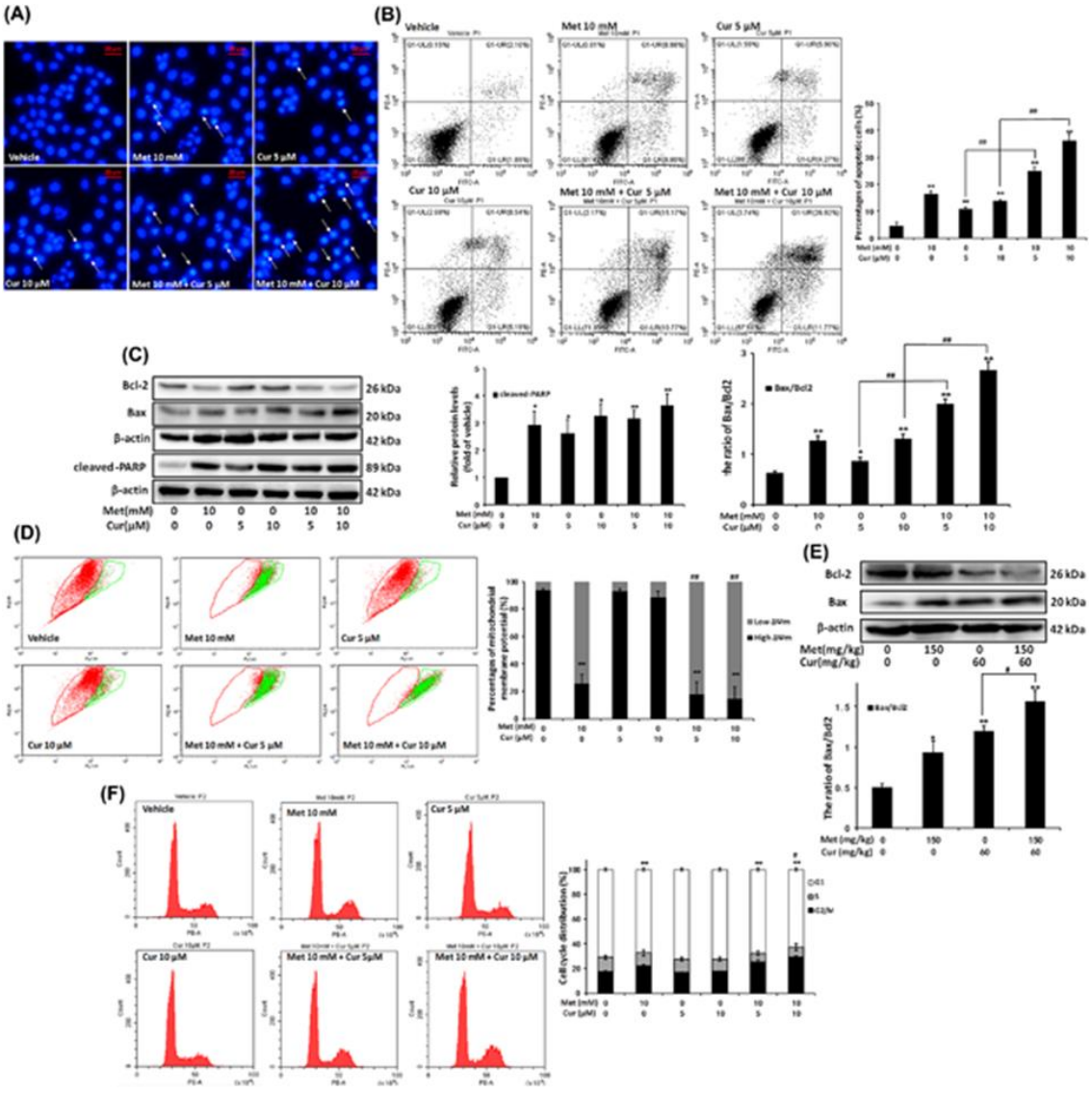
(A)
Vehicle
Met 10 mM
Cur 5 μM
Cur 10 μM
Met 10 mM + Cur 5 μM
Met 10 mM + Cur 10 μM
(B)
Vehicle
Met 10 mM
Cur 5 μM
Cur 10 μM
Met 10 mM + Cur 5 μM
Met 10 mM + Cur 10 μM
(C)
Bcl-2
Bax
β-actin
cleaved-PARP
β-actin
26 kDa
20 kDa
42 kDa
89 kDa
42 kDa
Met(mM) 0 10 0 0 10 10
Cur(μM) 0 0 5 10 5 10
(D)
Vehicle
Met 10 mM
Cur 5 μM
Cur 10 μM
Met 10 mM + Cur 5 μM
Met 10 mM + Cur 10 μM
(E)
Bcl-2
Bax
β-actin
26 kDa
20 kDa
42 kDa
Met(mg/kg) 0 150 0 150
Cur(mg/kg) 0 0 60 60
(F)
Vehicle
Met 10 mM
Cur 5 μM
Cur 10 μM
Met 10 mM + Cur 5μM
Met 10 mM + Cur 10 μM

Fig 5

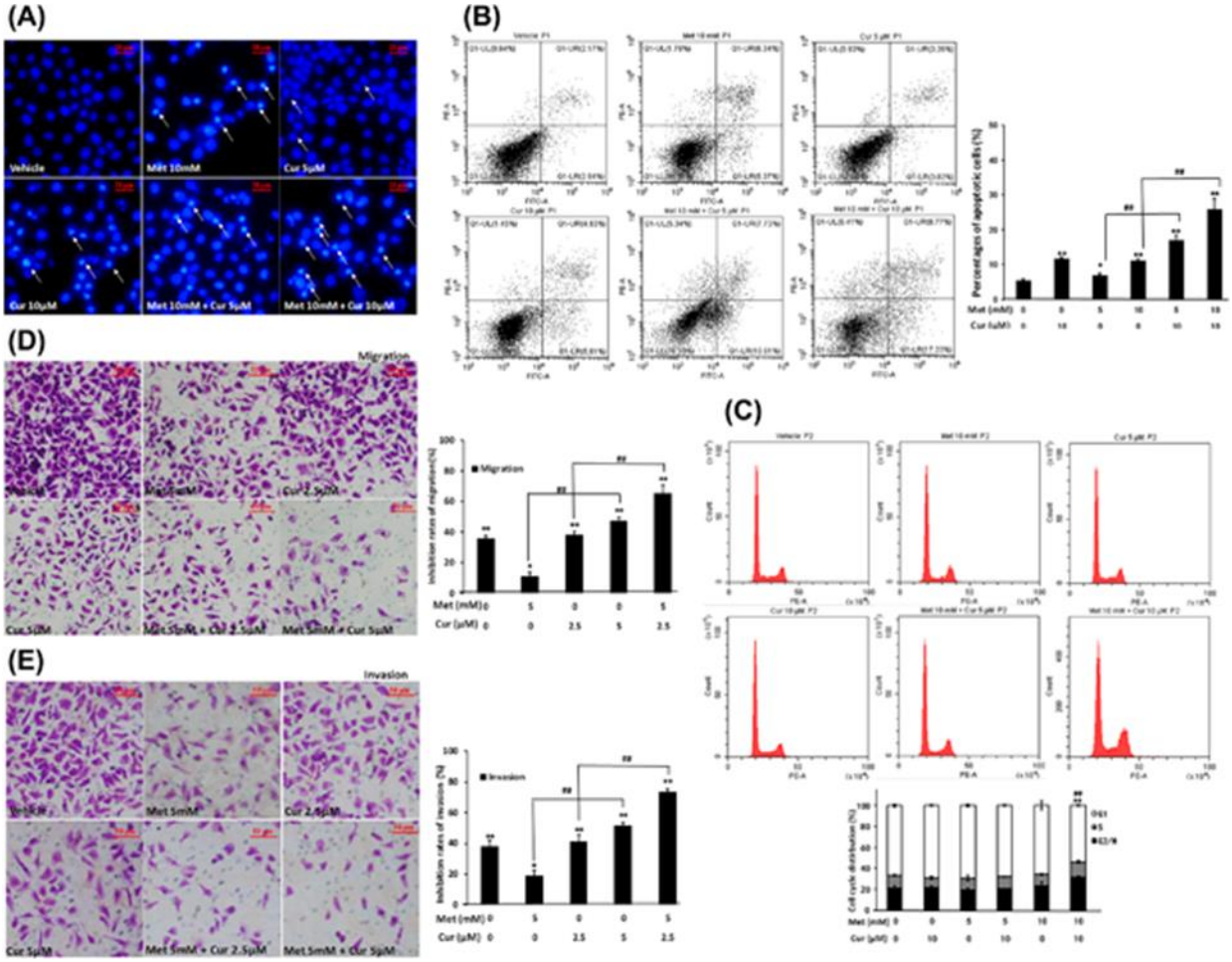
(A)
Vehicle
Met 10mM
Cur 5μM
Cur 10μM
Met 10mM + Cur 5μM
Met 10mM + Cur 10μM
(B)
Percentages of apoptotic cells (%)
(C)
(D)
Migration
Inhibition rates of migration(%)
(E)
Invasion
Inhibition rates of invasion (%)

Fig 6

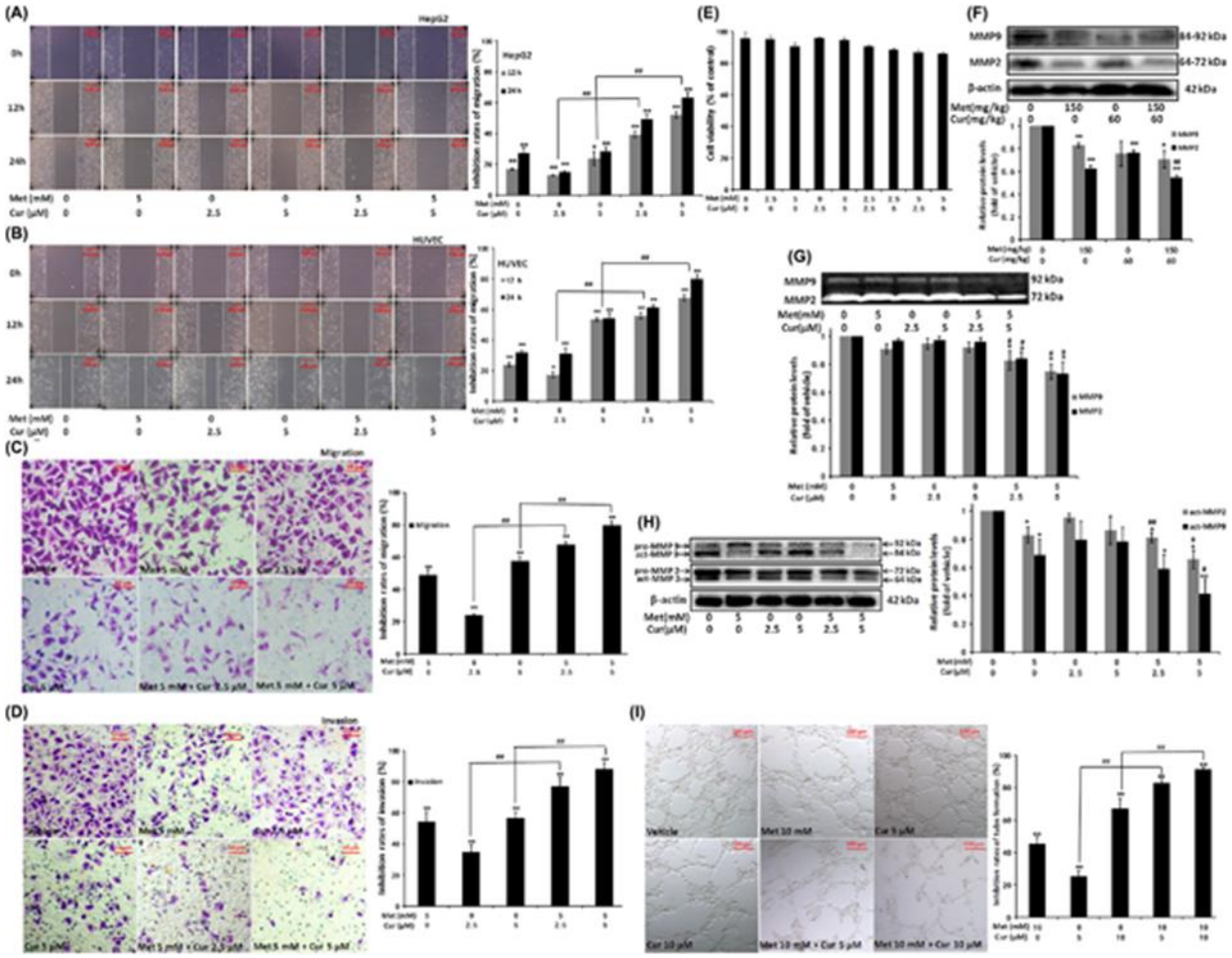
(A)
HepG2
0h
12h
24h
Met (mM) 0 5 0 0 5 5
Cur (μM) 0 0 2.5 5 2.5 5
HepG2
12 h
24 h
Inhibition rates of migration (%)
(E)
Cell viability (% of control)
(F)
MMP9
MMP2
β-actin
84-92 kDa
64-72 kDa
42 kDa
Met(mg/kg) 0 150 0 150
Cur(mg/kg) 0 0 60 60
MMP9
MMP2
Relative protein levels (fold of vehicle)
(B)
HUVEC
0h
12h
24h
Met (mM) 0 5 0 0 5 5
Cur (μM) 0 0 2.5 5 2.5 5
HUVEC
17 h
24 h
Inhibition rates of migration (%)
(G)
MMP9
MMP2
92 kDa
72 kDa
Met(mM) 0 5 0 0 5 5
Cur(μM) 0 0 2.5 5 2.5 5
MMP9
MMP2
Relative protein levels (fold of vehicle)
(C)
Migration
Vehicle
Met 5 mM
Cur 2.5 μM
Cur 5 μM
Met 5 mM + Cur 2.5 μM
Met 5 mM + Cur 5 μM
Migration
Inhibition rates of migration (%)
(H)
pro-MMP9
act-MMP9
92 kDa
84 kDa
pro-MMP2
act-MMP2
72 kDa
64 kDa
β-actin
42 kDa
Met(mM) 0 5 0 0 5 5
Cur(μM) 0 0 2.5 5 2.5 5
act-MMP2
act-MMP9
Relative protein levels (fold of vehicle)
(D)
Invasion
Vehicle
Met 5 mM
Cur 2.5 μM
Cur 5 μM
Met 5 mM + Cur 2.5 μM
Met 5 mM + Cur 5 μM
Invasion
Inhibition rates of invasion (%)
(I)
Vehicle
Met 10 mM
Cur 5 μM
Cur 10 μM
Met 10 mM + Cur 5 μM
Met 10 mM + Cur 10 μM
Inhibition rates of tube formation (%)

Fig 7

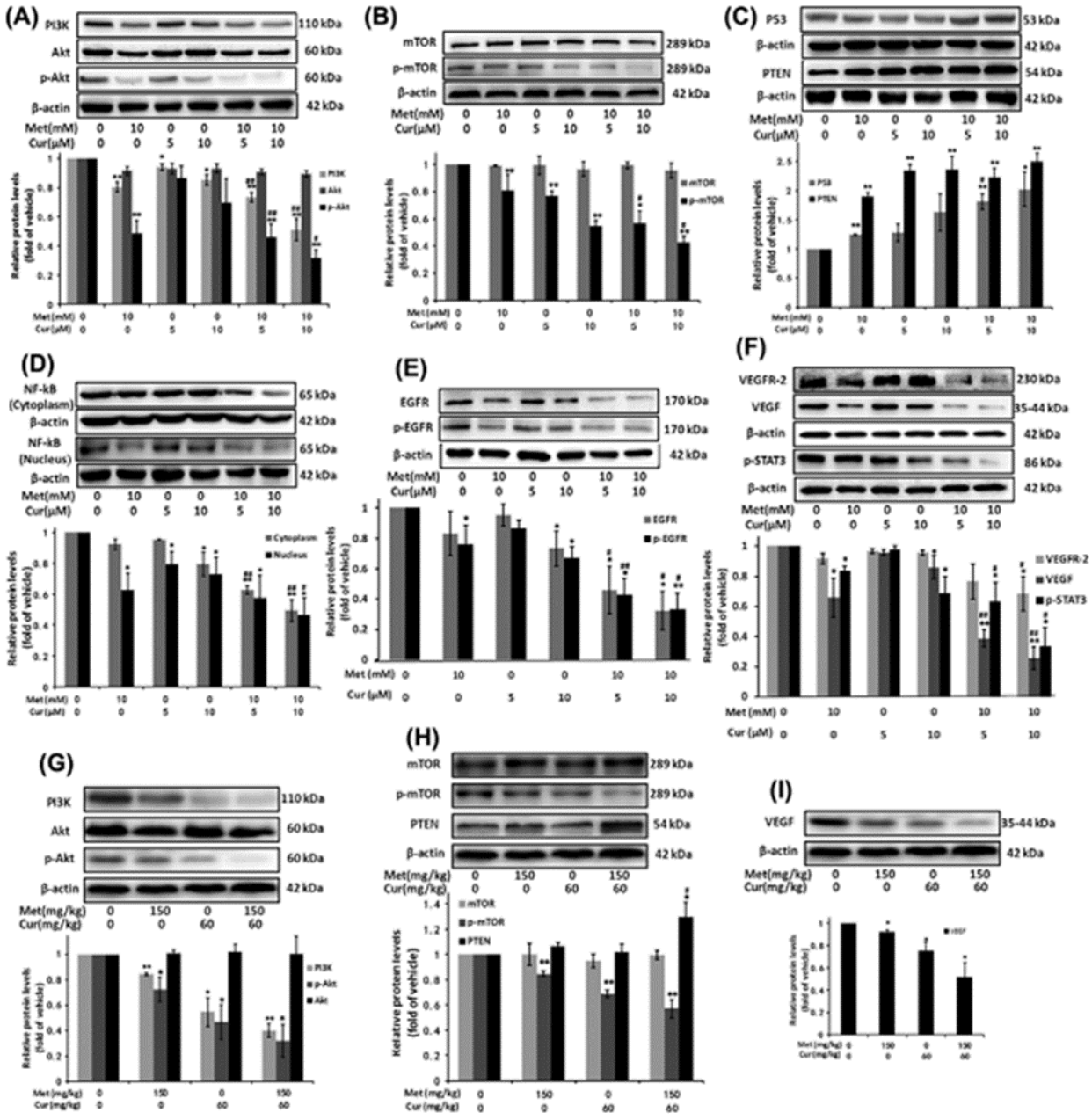
(A)
PI3K
Akt
p-Akt
β-actin
110 kDa
60 kDa
60 kDa
42 kDa
Met(mM) 0 10 0 0 10 10
Cur(μM) 0 0 5 10 5 10
Relative protein levels (fold of vehicle)
PI3K
Akt
p-Akt
(B)
mTOR
p-mTOR
β-actin
289 kDa
289 kDa
42 kDa
Met(mM) 0 10 0 0 10 10
Cur(μM) 0 0 5 10 5 10
Relative protein levels (fold of vehicle)
mTOR
p-mTOR
(C)
P53
β-actin
PTEN
β-actin
53 kDa
42 kDa
54 kDa
42 kDa
Met(mM) 0 10 0 0 10 10
Cur(μM) 0 0 5 10 5 10
Relative protein levels (fold of vehicle)
P53
PTEN
(D)
NF-kB (Cytoplasm)
β-actin
NF-kB (Nucleus)
β-actin
65 kDa
42 kDa
65 kDa
42 kDa
Met(mM) 0 10 0 0 10 10
Cur(μM) 0 0 5 10 5 10
Relative protein levels (fold of vehicle)
Cytoplasm
Nucleus
(E)
EGFR
p-EGFR
β-actin
170 kDa
170 kDa
42 kDa
Met(mM) 0 10 0 0 10 10
Cur(μM) 0 0 5 10 5 10
Relative protein levels (fold of vehicle)
EGFR
p-EGFR
(F)
VEGFR-2
VEGF
β-actin
p-STAT3
β-actin
230 kDa
35-44 kDa
42 kDa
86 kDa
42 kDa
Met(mM) 0 10 0 0 10 10
Cur(μM) 0 0 5 10 5 10
Relative protein levels (fold of vehicle)
VEGFR-2
VEGF
p-STAT3
(G)
PI3K
Akt
p-Akt
β-actin
110 kDa
60 kDa
60 kDa
42 kDa
Met(mg/kg) 0 150 0 150
Cur(mg/kg) 0 0 60 60
Relative protein levels (fold of vehicle)
PI3K
p-Akt
Akt
(H)
mTOR
p-mTOR
PTEN
β-actin
289 kDa
289 kDa
54 kDa
42 kDa
Met(mg/kg) 0 150 0 150
Cur(mg/kg) 0 0 60 60
Relative protein levels (fold of vehicle)
mTOR
p-mTOR
PTEN
(I)
VEGF
β-actin
35-44 kDa
42 kDa
Met(mg/kg) 0 150 0 150
Cur(mg/kg) 0 0 60 60

Fig 8

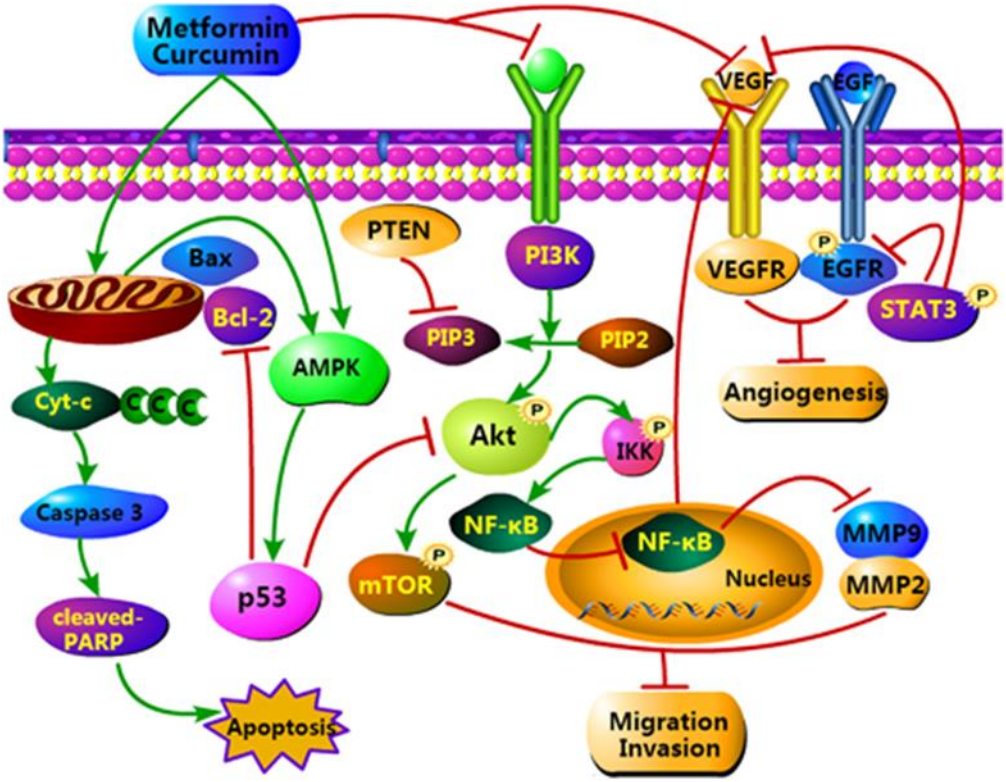
Metformin
Curcumin
VEGF
EGF
PTEN
PI3K
VEGFR
EGFR
STAT3
Bax
Bcl-2
PIP3
PIP2
AMPK
Angiogenesis
Cyt-c
Akt
IKK
Caspase 3
NF-κB
NF-κB
MMP9
MMP2
Nucleus
mTOR
p53
cleaved-
PARP
Apoptosis
Migration
Invasion

Table 1 The IC50 of metformin or curcumin on hepatoma cell lines

		IC_{50}	
Cell lines	**Time (h)**	**metformin (mM)**	**curcumin (μM)**
HepG2	24	53.72 ± 3.40	22.15 ± 0.51
	48	23.46 ± 3.45	15.94 ± 2.06
	72	8.52 ± 0.93	9.15 ± 0.20
PLC/PRF/5	24	63.62 ± 2.99	26.87 ± 2.46
	48	24.68 ± 0.55	16.33 ± 0.61
	72	9.97 ± 0.13	9.31 ± 0.95

Table 2 Combination index (CI) of metformin combined with curcumin on hepatoma cell lines

		CI	
Cell lines	**Curcumin (μM)**	**Metformin 5 mM**	**Metformin 10 mM**
HepG2	2.5	1.31	1.04
	5	1.03	0.76
	10	0.55	0.28
PLC/PRF/5	2.5	1.35	0.92
	5	1.15	0.66
	10	0.75	0.32

1.The CI = $(dA/DA) + (dB/DB)$, where dA and dB are the IC_{50} of compound A and B in combination, DA and DB are the IC_{50} of single compound A and B, respectively. CI values of <1, =1, and >1 indicated respectively synergism, additivity, and antagonism in combined agent action.

Table 3. The inhibitory effect of metformin and curcumin on HepG2 xenografts in nude mice (means ± SD, n = 7)

Group	Body weights (g) (Inbitiail/21days)	Tumor weight (g)	Tumor growth inhibition (%)
1. $^{**}P < 0.01$ versus vehicle group, $^{\#}P < 0.05$ versus Cur 60 mg/kg group.			
Vehicle	19.96 ± 0.51/21.56 ± 0.68	0.94 ± 0.33	-
Met 150 mg/kg	19.59 ± 1.12/21.00 ± 0.96	0.72 ± 0.27	24.10
Cur 60 mg/kg	19.03 ± 1.70/19.09 ± 1.73	0.64 ± 0.21	31.85
Met 150 mg/kg + Cur 60 mg/kg	19.76 ± 0.28/18.40 ± 1.15	0.39 ± 0.10$^{**,\#}$	58.33